Showcasing research from Dr Saines' laboratory, School of Natural Sciences, University of Kent, Kent, United Kingdom.

Analysis of a New Hydrochloride Salt of the Common Pharmaceutical Metformin

A dihydrochloride salt of the common pharmaceutical metformin has been reported and shown to be more soluble than the commercial monochloride salt. The work is the outcome of a community outreach project involving Year 12 A-level students, highlighting the value and significance of science performed in classroom environments.

Image reproduced by permission of Thomas J. Hitchings from *CrystEngComm,* 2025, **27**, 7785.

ROYAL SOCIETY
OF **CHEMISTRY**

rsc.li/crystengcomm

CrystEngComm

PAPER

Analysis of a new hydrochloride salt of the common pharmaceutical metformin

Thomas J. Hitchings,[a] School Project Students,[b] Angela Shepherd,[b]
Maria Alfredsson [ID][a] and Paul J. Saines [ID]*[a]

Metformin is a common active pharmaceutical ingredient and is usually administered orally in the solid form as a stable monohydrochloride salt. Herein, we discuss the crystal structure of a recently discovered dihydrochloride metformin salt, which reveals that protonation of the secondary amine in the divalent metformin cation disrupts both the extensive electron delocalisation and N–H⋯N hydrogen bonding found in the known α- and β-polymorphs of the metformin hydrochloride salt; this leads to charge-assisted N–H$^+$⋯Cl$^-$ hydrogen bonds dominating the solid form, forming a three-dimensional network. Analysis shows that metformin dihydrochloride can be distinguished from the metformin hydrochloride polymorphs by infrared spectroscopy and powder X-ray diffraction. Computational calculations suggest that metformin dihydrochloride has a lower lattice enthalpy than the known metformin hydrochloride phases, indicating a high solubility and lower stability consistent with experimental measurements.

Introduction

Metformin hydrochloride, the common name of *N,N*-dimethylbisguanidinium chloride, is a common medicine widely used to treat type-II diabetes by regulating blood glucose levels, with the exact mechanism still not understood.[1,2] It has also been used to improve pregnancy rates and as a potential cancer treatment.[3–5] Metformin's benefits as a treatment for various conditions do come with limitations, with a significant fraction of the >120 million patients worldwide experiencing adverse side effects.[6] When taken orally, α-metformin hydrochloride, which has high water solubility, is absorbed in the lower intestine but has relatively low bioavailability (50–60%) due to poor permeability across cell membranes;[6,7] this leads to classification as a Biopharmaceutics Classification System class III drug and requires larger doses. Reported side effects, broadly described as gastrointestinal intolerances (GI), vitamin deficiencies and low blood sugar, have been linked to the high solubility and fast release time of the drug.[8] While the precise mechanism by which GI intolerances occur remain unclear this may be linked to high local luminal concentrations that result from the high dosage needed, explaining why slow-release formulations reduce these side effects.[2] Whilst there has been advancement in active pharmaceutical ingredient (API) slow-release mechanisms as

part of the formulation of pharmaceuticals,[6,9] another impact on drug solubility and, therefore, release time is polymorphism and co-crystallisation.[10] These can affect a range of properties, including drug solubility, dissolution rates, hygroscopy, and long-term stability.[11,12] In extreme cases different polymorph solubility can lead to mass recalls of solid-form pharmaceuticals, as occurred for ritonavir in 1998 due to a more stable polymorph with lower solubility and reduced bioavailability.[13]

The diversity of structures in the solid form can be categorised into single or multiple-component crystals. Those that contain multiple components can be classified as salts, solvates or co-crystals, with each able to form polymorphs.[14] The interactions between molecules usually dictate the deviations in packing between polymorphs. The number and ratio of hydrogen bond donors and acceptors can influence the formation of different solid forms, as can changes in molecular shape due to rotations around dihedral angles. 5-Methyl-2-[(2-nitrophenyl)amino]-3-thiophenecarbonitrile, commonly known as ROY, is a system famed for its myriad polymorphs with over 15 known polymorphs and counting.[15–17] The strength of hydrogen bonding also plays a role in system susceptibility to forming a diverse range of structures. Charge-assisted hydrogen bonding introduces ionicity to the hydrogen bond, where the donor and acceptor species carry a positive and/or negative charge.[18,19] Examples of these can be found in molecular salts and co-crystals, including pharmaceuticals.[19,20] Interactions between positively charged protonated hydrogen bond donors and chloride anions sit in the murky in-between of ionic bonds,

[a] *Chemistry and Forensic Science, School of Natural Sciences, Ingram Building, University of Kent, Canterbury, Kent, CT2 7NH, UK. E-mail: P.Saines@kent.ac.uk*
[b] *Simon Langton Girls' Grammar School, Canterbury, Kent, CT1 3EW, UK*

strong dipole–dipole interaction, and hydrogen bonds. However, for the purpose of this study, they are considered charge-assisted hydrogen bonds.[18,19]

Metformin hydrochloride has two known polymorphs, α and β, with the latest reported in 2004.[21,22] The two polymorphs are monoprotic with the secondary amine site deprotonated, leading to delocalisation of the π electrons and consequently resonance structures.[22,23] The two polymorphs crystallise in $P2_1/c$ and show differences in crystal packing, which leads to differences in physical properties.[21,22] Co-crystals have already been explored, with metformin citrate showing improved stability compared to α-metformin hydrochloride.[24] Metformin has also been found as diprotic when co-crystallised with *N,N'*-(1,4-phenylene)dioxalamic acid, and found to show charge assisted intermolecular interactions.[25] Herein, we discuss a new salt, metformin dihydrochloride, in which the metformin is diprotic as an extension of the pharmaceutically relevant metformin hydrochloride compounds. We first crystallised metformin dihydrochloride as part of a local outreach project. In parallel to our efforts, Xia[26] reported the X-ray crystal structure but without detailed discussion or further characterisation. We have subsequently obtained a sample of the material of suitable purity for bulk characterisation by common methods that would enable it to be distinguished from the related monoprotonated phases. We have also completed computational studies that suggest it is likely more soluble and less stable than the monoprotonated chloride salts, which is supported by experimental measurements. The greater solubility of metformin dihydrochloride may worsen GI side effects should samples of α-metformin hydrochloride be contaminated with it.

Experimental

Colourless single crystals of metformin dihydrochloride were produced by the dissolution of α-metformin hydrochloride with stoichiometric amounts of 2 M hydrochloric acid. This was then recrystallised at room temperature over several months. Phase purity was initially assessed using a pattern collected on a Rigaku Miniflex diffractometer using Cu K_α, with a fit to the pattern obtained using the Le Bail method as implemented in GSAS-II indicating that metformin dihydrochloride is the main phase present along with a small amount of the α-polymorph (see Fig. S1).[27] Microanalysis results also confirm a bulk composition consistent with metformin dihydrochloride (see Table S1).

Crystals were mounted in Fromlin oil onto a MiTeGen microloop attached to the 3-circle goniometer of the Rigaku Supernova diffractometer. An Oxford cryostream 800+ was used to cool the crystal to 100 K. X-rays were generated using a Mo K_α microfocus tube with diffraction measured using an ATLAS CCD detector. Data processing was carried out using Crysalis Pro,[28] with structure solution performed with SHELXS Direct methods in the Olex-2 interface.[29,30] Structural refinements were performed using SHELXL with

hydrogens added at geometrically calculated positions after their location in difference electron-density maps.[31]

Thermal analysis was performed using the NETZSCH 409 PG/PC TGA with thermogravimetric analysis (TGA) and differential scanning calorimetry (DSC) collected in parallel. Samples were loaded into ceramic crucibles and heated under air at an average rate of 10 °C min^{-1}. Fourier transform infrared spectroscopy (FTIR) was conducted and averaged over 32 scans using the Shimadzu IRAffinity-1S Fourier transform spectrometer equipped with an attenuated total reflection stage.

Computational evaluation of the α-metformin monohydrochloride and metformin dihydrochloride was completed using BIOVIA Materials Studio 2022 with the CASTEP[32] module and CrystalExplorer21.[33] The calculation was performed on each polymorph and salt using the GGA BLYP functional with the pseudopotentials, which were allowed to converge over a single gamma point with a DFT-d Grimme semi-empirical dispersion correction following an LBFGS geometry optimisation of the crystallographic models.[34] The plane wave OTFG ultrasoft pseudopotential basis set was used with an energy cut-off set to 570 eV and no periodic dipole correction. Values for lattice energy, E_{latt}, are calculated by eqn (1):

$$E_{latt} = E_{crystal}^{total} - ZE_{molecule}^{total} \tag{1}$$

where Z refers to the number of asymmetric units in the unit cell. The calculation of $E_{molecule}$ was performed in the same manner as before, on a single asymmetric unit in a 25 Å × 25 Å × 25 Å cell.

Analysis in CrystalExplorer21 consisted of generating Hirschfeld surfaces to compare molecular packing between the two monochloride polymorphs and dichloride salt as well as using DFT with the CE-B3LYP function as implemented in CrystalExplorer21 to calculate interaction energies and, subsequently, the lattice energies of the salts as a proxy to indicate differences in solubility. Lattice energies in CrystalExplorer21 (ref. 33) are calculated on >20 Å sized clusters as half the summation of interactions between the central molecule with another in the cluster, using eqn (2) and (3):

$$E_{latt} = \frac{1}{2} \sum_{Pairs} E_{total} + E_{cell\ dipole} \tag{2}$$

$$E_{cell\ dipole} = \frac{-2\pi\rho_{cell}^2}{3ZV_{cell}} \tag{3}$$

as described by Thomas *et al.*[35] The average discrepancies between the calculated and measured values have historically been no more than 7 kJ mol^{-1} at a maximum.[35] Coulombic interaction energies are combined with dispersion and repulsion energies as corrections to the total energy to give the lattice energy. Interaction energies are calculated as columbic interaction energies.

Results and discussion

Crystal structure

Metformin dihydrochloride crystallises in the polar monoclinic space group $P2_1$; full crystallographic details are presented in Table S2. Variable temperature single crystal X-ray diffraction shows no sign of any phase transitions between 100–300 K, with the monoclinic cell distortion modestly decreasing with increasing temperature (see Fig. S2 with thermal expansion coefficients in Table S3). The asymmetric unit consists of diprotic metformin with all nitrogen groups 3-coordinate and two chloride anions for charge balance, see Fig. 1. Compared to the monohydrochloride polymorphs, this dichloride salt has its secondary amine protonated in addition to all primary amines. The C1–N3–C2–N5 torsion angle ($\varphi°$) of the

Fig. 1 Asymmetric unit of (top) metformin dihydrochloride, (middle) α-metformin hydrochloride and (bottom) β-metforminhydrochloride.[21,22]

dichloride salt is 139.5(4)° and is closer to a planar configuration than the monoprotic forms (α = 56.5(5)° and β = 129.1(2)°). This is also in line with diprotic metformin citrate being more planar, showing a torsion angle of 148.8(8)°.[25]

A charge density study of the monoprotic α form showed that metformin is protonated on the primary amine functional groups, with the N3 secondary amine site deprotonated.[23] It suggested extensive electron delocalisation across the metformin molecule with only the C–N bonds to the tertiary N site being single bonds and the highest bond orders being associated with the C–N bonds to the secondary amine, N3. In contrast analysis of the bond distances, presented in Table S4, indicates that the C–N bonds to the secondary amine are significantly lengthened in the dichloride salt compared to both monoprotic salts while the C–N bonds to the primary amines (N1/N2–C1 and N4–C2) are shorter than in the monoprotic salts.[22,23] This suggests the π-bonding of the diprotic metformin is disrupted by the protonation of the secondary amine (N3), resulting in a distinct resonance structure from the monoprotic forms. The bond distances to the methyl groups are consistent across all three forms suggesting these remain single bonds.

In the dichloride phase, the metformin is packed into a 3D hydrogen bond networked structure with neighbouring cations along the c-axis shifted by half a unit cell. This is in contrast with the hydrogen-bonded chains of metformin molecules adopted by the α-form and the dimerisation of metformin molecules that are found in the β-polymorph. The key difference in the intermolecular interactions between the monochloride compounds and the new dichloride salt arises from the latter having a larger ratio of chloride anions to metformin molecules and a protonated N3 site that makes it less favourable as a hydrogen bond acceptor site. In the α- and β-monochloride forms, there is a combination of charge-assisted hydrogen bonding and intermolecular hydrogen bonding between their metformin molecules, the latter involves the N3 site acting as a hydrogen acceptor. In contrast, in metformin dihydrochloride the molecules pack with only charge-assisted hydrogen bonds between N–H groups and chloride anions, N–H$^+\cdots$Cl$^-$ (see Fig. S3 for packing diagram). Charge-assisted hydrogen bonds form with both Cl1 and Cl2 (full details of hydrogen bonding interactions can be found in Table S5). Cl1 is involved in three hydrogen bonds, two involving one metformin cation *via* interactions with the hydrogen bound to the N2 and N4 sites and another with the other distinct proton on the N4 site on an adjacent cation. Cl2 is involved with four hydrogen bonds, two with protons bonded to hydrogen atoms on N1 and N2 with two further hydrogen bonds to other metformin molecules; one with the other distinct proton on another N2 and a second with the proton bonded to N3. This results in all protons bonded to an amine being involved in a single charge-assisted hydrogen bond. The N3–H3$^+\cdots$Cl2 donor–acceptor distance is classified as unusually short (see Table S6 and Fig. S4 for further details) using the 'Hydrogen Bond
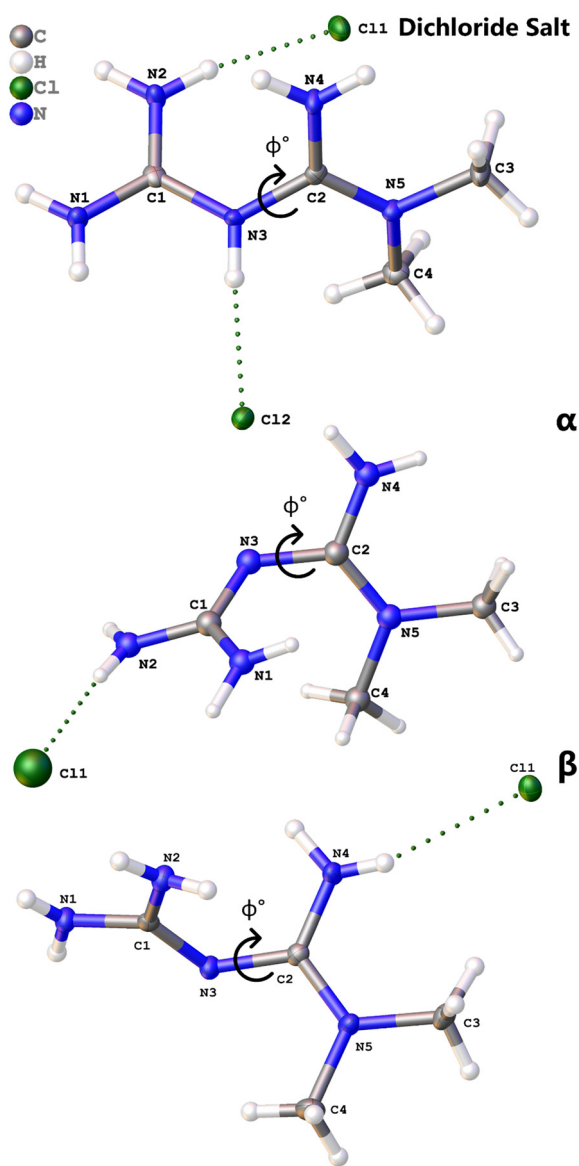
Statistics' tool in the Materials package of the Mercury programe.[36,37] This may suggest the N3 site is overbonded in the structure such that it is favourable for the hydrogen associated with it to form a stronger hydrogen bond.

The interactions in the dichloride salt have been analysed using Hirschfeld surfaces and summarised as fingerprint plots (see Fig. 2 and S5 for further breakdown). These indicate that Cl···H interactions comprise 30.9% of contacts in the dichloride form compared to 14.4% in the alpha and 15.6% in the beta monohydrochloride compounds. The fingerprint plots also confirm the limited amount of N···H interactions in the metformin dihydrochloride salt (7.2% of contacts), which show up as pseudosymmetric 'wings' on the fingerprint plots of the α (16.3% of contacts) and β (16.6% of contacts) forms. This further confirms the dominance of charge assisted hydrogen bonding interactions in the dichloride salt compared to the monochloride compounds.

Bulk analysis

Physical characterisation of metformin dihydrochloride compared to the physical properties of α-metformin hydrochloride show that these are readily distinguishable by standard laboratory analysis. Simulated powder patterns for each of the three known phases, α, β and dichloride salt, (see Fig. S6), show that these phases are clearly distinguishable with minimal peak overlap.[22] FTIR spectra shows a clear increase in intensity in the broad N–H stretch at ~2700 cm^{-1} in the diprotic metformin hydrochloride compared to the monoprotic metformin hydrochloride (see Fig. 3). This is usually associated with amine salts and would be expected to increase given the increased number of charge assisted hydrogen bond interactions.[38] The combination of protonated primary and secondary amine groups in the dichloride results in broader features between 3500–2800 cm^{-1} due to overlapping peaks from the different N–H stretches. Combinations of C=N and C–N stretches are observed strongly in both compounds between 1600–1200 cm^{-1} but at differing positions. This supports the idea that the monoprotic and diprotic metformin molecules show different resonance structures but could also be influenced by differing contributions from N–H bending modes, which are usually observed around 1500–1650 cm^{-1}.

Thermal analysis shows differences in thermal stability between phases with an endothermic process occurring at ~210 °C for metformin dihydrochloride and ~230 °C for α-metformin hydrochloride (see Fig. 4), the latter matches with literature values.[12,39] This would suggest that the dichloride salt is less thermally stable than the α form.[40,41] The α-metformin hydrochloride has a sharper endothermic peak in its calorimetry measurement than the metformin dihydrochloride salt complex, which may suggest the latter has a more complex degradation. An approach to estimating the stability of a polymorph based on the difference in density between polymorphs was used previously when the β form was reported, where it was suggested that a difference in density of 5% between forms indicated the α-polymorph was more stable. The difference in density between the α form and the dichloride compound is approximately 2%, suggesting this former is the more stable form, particularly given the higher chloride content of the latter phase.[22,42] Despite this powder X-ray diffraction patterns collected of the metformin dihydrochloride remained similar after 2 years of
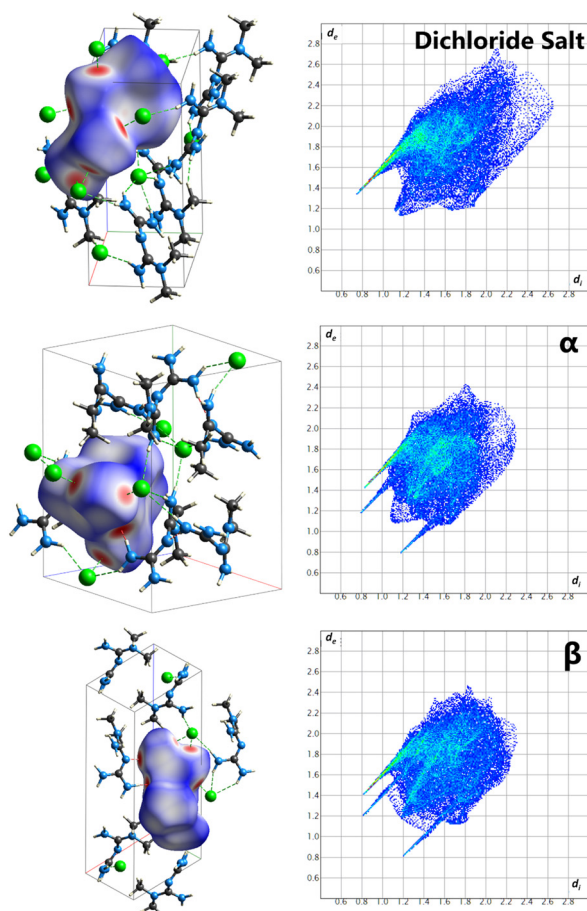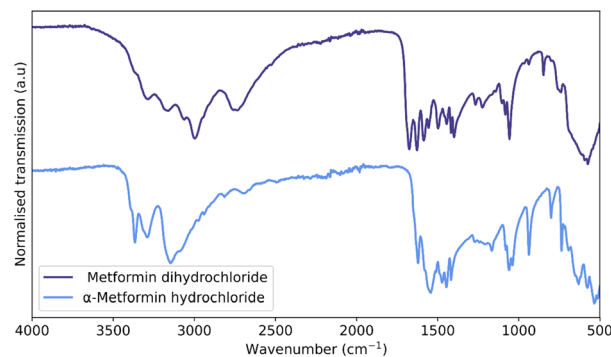

Fig. 2 The Hirschfeld surfaces and respective fingerprint plots generated around each metformin molecule for (top) metformin dihydrochloride, (middle) α-metformin hydrochloride, (bottom) β-metformin hydrochloride.

Fig. 3 Normalised FTIR of metformin dihydrochloride (dark blue) and α-metformin hydrochloride (light blue) offset for clarity.
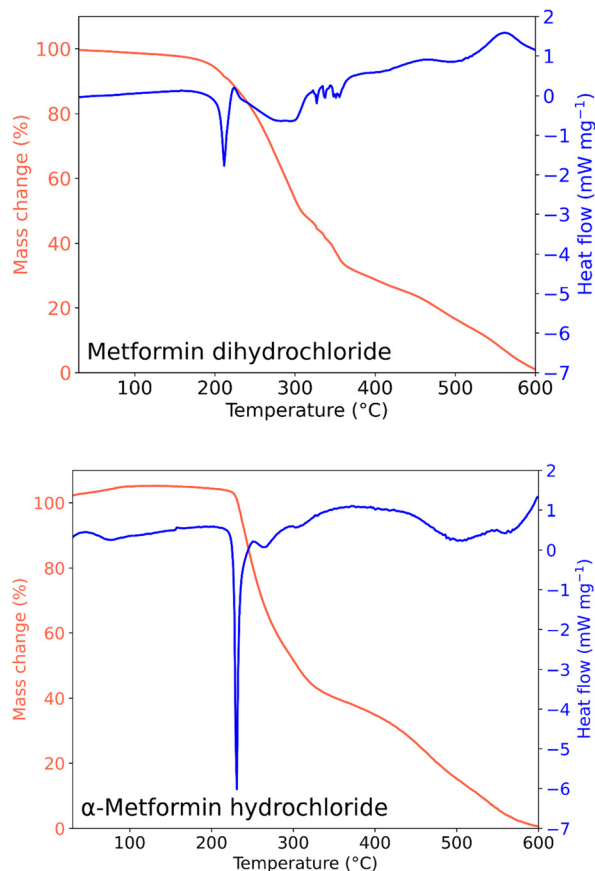
Fig. 4 Thermal gravimetric analysis and simultaneous differential scanning calorimetry for (top) metformin dihydrochloride and (bottom) α-metformin hydrochloride.

energies are comparable to the measured enthalpy of sublimation, eqn (1) and (2).[35,43] Independent of the method lattice energy calculations suggest that metformin dihydrochloride has a significantly smaller lattice energy than either monochloride form (see Table 1), suggesting it is the least energetically stable of these three forms. The CrystalExplorer calculations have the caveat that non-centrosymmetric structures with polar point groups require a more significant cell dipole energy ($E_{cell\ dipole}$) correction to the calculation, eqn (3), which is usually a small, insignificant effect for non-polar structures. Metformin dihydrochloride is a polar structure, so its lattice energy will be heavily dependent on the shape of the crystal, and, as such, the lattice energy determined is an approximation for an individual crystal.[44] Some typical values of $E_{cell\ dipole}$ for polar structures are −17.9 kJ mol^{-1} and −24.6 kJ mol^{-1}, respectively, for HF and HCN, introducing a broader correction on the calculated values.[35] The larger size of the metformin molecule will significantly reduce the density of dipoles and therefore likely the size of this correction compared to these simple inorganic structures, although this may be somewhat offset by the charge on it that results from protonation. Calculating the lattice energies using a periodic mode in CASTEP avoids the issues with the dipole moment correction. While these DFT methods traditionally do not calculate hydrogen bonding and van der Waals forces accurately the use of the Grimme-D correction,[34] which introduces dispersion forces in the structure, compensates for this. This correction is likely the cause of the higher interaction energies from the CASTEP calculations as opposed to those obtained using CrystalExplorer.

The calculations in CrystalExplorer are also visualised as energy frameworks showing the directionality and relative strength of the interactions, which suggest the interactions in the metformin dihydrochloride phase is more uniform in three dimensions than is the case for the α and β phases (see Fig. S8). This is consistent with the three-dimensional hydrogen bonding network we describe for the dihydrochloride phase. These calculations suggest the interactions between the metformin and Cl2 environment are more significant than the interactions with the Cl1 site.

The smaller calculated lattice energies of the dihydrochloride salt indicate it would require a less endothermic dissolution process and thus be more soluble than both the α- and β-metformin hydrochloride polymorphs. The smaller lattice enthalpy is likely due to the packing being dominated by the more ionic charge assisted hydrogen bonds

storage under ambient conditions, with no new phases found to form over this period of time (see Fig. S7).

Computational analysis

We anticipate that the monoprotonated and diprotonated metformin cations would rapidly interchange in solutions in the body due to the loss or addition of the highly labile protons associated with the amine groups. The form present will primarily be dependent on pH and thus the permeability across cell membranes likely remains similar regardless of the solid form it originates from. Thus the pharmacological implications of metformin dihydrochloride are primarily with regards to its solubility. Thus to estimate the solubility of these compounds, interactions are calculated as lattice energies using both CrystalExplorer and CASTEP. For a molecular salt such calculated lattice

Table 1 The lattice energies calculated using CASTEP and CrystalExplorer21

Method	α-Metformin hydrochloride/ kJ mol^{-1}	β-Metformin hydrochloride/ kJ mol^{-1}	Metformin dihydrochloride/ kJ mol^{-1}
CASTEP, BLYP	−108.91	−109.00	−63.61
CrystalExplorer21, CE-B3LYP, >20 Å cluster	−96.90	−94.35	−41.50

with no N–H⋯N hydrogen bonding possible due to the lack of H-bond acceptors on the doubly protonated metformin cation. This is reasonable with charge-assisted X–H$^+$⋯Cl$^-$ hydrogen bonds found to be weaker than conventional hydrogen bonding interactions.[18,19,45] Our calculations in CASTEP confirm the weaker nature of the charge-assisted N–H$^+$⋯Cl$^-$ hydrogen bonds, indicating these have a bond energy of −1132 kJ mol^{-1} compared to the N–H⋯N bond energy of 17.9 kJ mol^{-1}. They also indicate the N–H$^+$⋯Cl$^-$ interaction being more stable in its ionic form where the positive charge is primarily associated with the proton rather than being delocalised across the N–H bond by approximately 1067 kJ mol^{-1}. Consistent with the proposed higher solubility of metformin dihydrochloride experimental solubility measurements suggested metformin dihydrochloride is roughly twice as soluble as α-metformin hydrochloride. This is based on visual observation of 31 mg of metformin dihydrochloride and α-metformin hydrochloride dissolving in 20 μL and 40 μL of ultrapure water, respectively, at 20 °C with intermittent sonication and solution added in 10 μL aliquots. These calculations also match well with the experimentally observed degradation temperatures, which show that the dichloride salt is less stable and has a lower density Undesirable side effects from metformin hydrochloride, such as gastrointestinal intolerances, have been linked to fast release times due to its high solubility, with slow release technologies utilised to mitigate these.[2] Thus, being able to identify any contamination from metformin dihydrochloride, which could arise through accidental addition of excessive HCl, is vital to avoid worsening these side effects.

Conclusions

Our analysis of the structure of metformin dihydrochloride, a new salt of the pharmaceutical metformin hydrochloride, indicates the second proton is accommodated on the secondary amine site. This disrupts the extensive electron delocalisation found in the monovalent form and eliminates N–H⋯N hydrogen bonds that play a role in the known metformin hydrochloride forms such that only charge assisted N–H$^+$⋯Cl$^-$ hydrogen bonds exist between the divalent metformin molecules leading to a three-dimensional hydrogen bond network. This work shows that the existence of the metformin dihydrochloride can be readily identified by both infrared spectra and powder X-ray diffraction, enabling the potential for contamination of pharmaceutical samples to be avoided. Experimental analysis and computational calculations suggest this is a less stable form of metformin hydrochloride with a lower decomposition temperature and higher solubility and potentially different pharmacokinetics. This new salt was synthesised as part of an outreach project involving an extensive crystal screening and highlights the potential and rise in such public engagement activities to advance scientific understanding.[46]

Author contributions

This project was conceived by PJS and TJH, with PJS and AS responsible for funding acquisition. Sample synthesis was performed by the school project students under the supervision of TJH and AS. Crystallographic experiments and bulk characterisations were collected and formally analysed by TJH and supervised by PJS. TJH performed computational calculations under the supervision of MA. Writing the original draft was done by TJH, and TJH, PJS and MA were responsible for reviewing and editing.

Conflicts of interest

There are no conflicts of interest to declare.

Data availability

Data for this article, including diffraction patterns, elemental analysis and combined thermogravimetric differential scanning calorimetry measurements, are available at the Kent Data Repository at https://data.kent.ac.uk/id/eprint/579.

Supplementary information: the list of school project students who have given permission to be named as authors of this work and further crystallographic details, computational analysis and bulk composition results are presented as plots and tables. See DOI: https://doi.org/10.1039/d5ce00711a.

CCDC 2404113 contains the supplementary crystallographic data for this paper.[47]

Acknowledgements

Notes and references

1 U. Hostalek and I. Campbell, *Curr. Med. Res. Opin.*, 2021, **37**, 1705–1717.
2 G. Rena, D. G. Hardie and E. R. Pearson, *Diabetologia*, 2017, **60**, 1577–1585.
3 X. Sui, Y. Xu, X. Wang, W. Han, H. Pan and M. Xiao, *Mol. Pharmaceutics*, 2015, **12**, 3783–3791.
4 V. N. Sivalingam, J. Myers, S. Nicholas, A. H. Balen and E. J. Crosbie, *Hum. Reprod. Update*, 2014, **20**, 853–868.
5 S. R. Lord and A. L. Harris, *Br. J. Cancer*, 2023, **128**, 958–966.
6 M. Cetin and S. Sahin, *Drug Delivery*, 2016, **23**, 2796–2805.
7 X. Gu, Z. Si, Y. Yan and X. Zhang, *Int. J. Pharm.*, 2022, **616**, 121517.
8 L. O. Tso, M. F. Costello, L. E. T. Albuquerque, R. B. Andriolo and C. R. Macedo, *Cochrane Database Syst. Rev.*, 2020, **12**, CD006105.
9 L. M. Martin and A. R. Rajabi-Siahboomi, *AAPS Adv. Pharm. Sci. Ser.*, 2014, **16**, 123–141.

10 E. H. Lee, *Asian J. Pharm. Sci.*, 2014, **9**, 163–175.

11 X. Sun, S. Du, Y. Sun, H. Li, C. P. Yu, J. Guo, Y. Wang, S. Yu, Y. Cheng and F. Xue, *J. Chem. Eng. Data*, 2021, **66**, 3282–3292.

12 I. Benmessaoud, O. Koutchoukali, M. Bouhelassa, A. Nouar and S. Veesler, *J. Cryst. Growth*, 2016, **451**, 42–51.

13 S. R. Chemburkar, J. Bauer, K. Deming, H. Spiwek, K. Patel, J. Morris, R. Henry, S. Spanton, W. Dziki, W. Porter, J. Quick, P. Bauer, J. Donaubauer, B. A. Narayanan, M. Soldani, D. Riley and K. McFarland, *Org. Process Res. Dev.*, 2000, **4**, 413–417.

14 S. Aitipamula, R. Banerjee, A. K. Bansal, K. Biradha, M. L. Cheney, A. R. Choudhury, G. R. Desiraju, A. G. Dikundwar, R. Dubey, N. Duggirala, P. P. Ghogale, S. Ghosh, P. K. Goswami, N. R. Goud, R. R. K. R. Jetti, P. Karpinski, P. Kaushik, D. Kumar, V. Kumar, B. Moulton, A. Mukherjee, G. Mukherjee, A. S. Myerson, V. Puri, A. Ramanan, T. Rajamannar, C. M. Reddy, N. Rodriguez-Hornedo, R. D. Rogers, T. N. G. Row, P. Sanphui, N. Shan, G. Shete, A. Singh, C. C. Sun, J. A. Swift, R. Thaimattam, T. S. Thakur, R. Kumar Thaper, S. P. Thomas, S. Tothadi, V. R. Vangala, N. Variankaval, P. Vishweshwar, D. R. Weyna and M. J. Zaworotko, *Cryst. Growth Des.*, 2012, **12**, 2147–2152.

15 S. Chen, I. A. Guzei and L. Yu, *J. Am. Chem. Soc.*, 2005, **127**, 9881–9885.

16 L. Yu, *Acc. Chem. Res.*, 2010, **43**, 1257–1266.

17 A. Lévesque, T. Maris and J. D. Wuest, *J. Am. Chem. Soc.*, 2020, **142**, 11873–11883.

18 J. O. Lundgren and I. Olovsson, *Acta Crystallogr.*, 1967, **23**, 966–971.

19 T. Steiner, *Angew. Chem., Int. Ed.*, 2002, **41**, 48–76.

20 D. J. Berry and J. W. Steed, *Adv. Drug Delivery Rev.*, 2017, **117**, 3–24.

21 M. Hariharan, S. S. Rajan and R. Srinivasan, *Acta Crystallogr., Sect. C: Cryst. Struct. Commun.*, 1989, **45**, 911–913.

22 S. L. Childs, L. J. Chyall, J. T. Dunlap, D. A. Coates, B. C. Stahly and G. P. Stahly, *Cryst. Growth Des.*, 2004, **4**, 441–449.

23 R. N. Devi, C. Jelsch, S. Israel, E. Aubert, C. Anzline and A. A. Hosamani, *Acta Crystallogr., Sect. B: Struct. Sci., Cryst. Eng. Mater.*, 2017, **73**, 10–22.

24 C. Verdugo-Escamilla, C. Alarcón-Payer, F. J. Acebedo-Martínez, A. Domínguez-Martín and D. Choquesillo-Lazarte, *Crystals*, 2022, **12**, 1748.

25 S. Chong-Canto, E. V. García-Báez, F. J. Martínez-Martínez, A. A. Ramos-Organillo and I. I. Padilla-Martínez, *Pharmaceutics*, 2020, **12**, 998.

26 Y. P. Xia, *Z. Kristallogr. – New Cryst. Struct.*, 2023, **238**, 799–800.

27 B. H. Toby and R. B. Von Dreele, *J. Appl. Crystallogr.*, 2013, **46**, 544–549.

28 *Crysalis Pro V.171.38.43*, Rigaku Oxford Diffraction, 2016.

29 O. V. Dolomanov, L. J. Bourhis, R. J. Gildea, J. A. K. Howard and H. Puschmann, *J. Appl. Crystallogr.*, 2009, **42**, 339–341.

30 G. Sheldrick, *Acta Crystallogr., Sect. A: Found. Crystallogr.*, 2008, **64**, 112–122.

31 G. M. Sheldrick, *Acta Crystallogr., Sect. C: Struct. Chem.*, 2015, **71**, 3–8.

32 S. J. Clark, M. D. Segall, C. J. Pickard, P. J. Hasnip, M. I. J. Probert, K. Refson and M. C. Payne, *Z. Kristallogr.*, 2005, **220**, 567–570.

33 P. R. Spackman, M. J. Turner, J. J. McKinnon, S. K. Wolff, D. J. Grimwood, D. Jayatilaka and M. A. Spackman, *J. Appl. Crystallogr.*, 2021, **54**, 1006–1011.

34 S. Grimme, *J. Comput. Chem.*, 2004, **25**, 1463–1473.

35 S. P. Thomas, P. R. Spackman, D. Jayatilaka and M. A. Spackman, *J. Chem. Theory Comput.*, 2018, **14**, 1614–1623.

36 C. R. Groom, I. J. Bruno, M. P. Lightfoot and S. C. Ward, *Acta Crystallogr., Sect. B: Struct. Sci., Cryst. Eng. Mater.*, 2016, **72**, 171–179.

37 C. F. Macrae, I. Sovago, S. J. Cottrell, P. T. A. Galek, P. McCabe, E. Pidcock, M. Platings, G. P. Shields, J. S. Stevens, M. Towler and P. A. Wood, *J. Appl. Crystallogr.*, 2020, **53**, 226–235.

38 B. Smith, *Infrared spectral interpretation: A systematic approach*, CRC Press Taylor & Francios Group, 1st edn, 2018.

39 S. Ramukutty, R. Jeyasudha and E. Ramachandran, *J. Pharm. Pharm. Sci.*, 2014, **3**, 36–40.

40 N. Schultheiss and A. Newman, *Cryst. Growth Des.*, 2009, **9**, 2950–2967.

41 E. Batisai, A. Ayamine, O. E. Y. Kilinkissa and N. B. Báthori, *CrystEngComm*, 2014, **16**, 9992–9998.

42 A. Gavezzotti and G. Filippini, *J. Am. Chem. Soc.*, 1995, **117**, 12299–12305.

43 C. F. Mackenzie, P. R. Spackman, D. Jayatilaka and M. A. Spackman, *IUCrJ*, 2017, **4**, 575–587.

44 B. P. Van Eijck and J. Kroon, *J. Phys. Chem. B*, 1997, **101**, 1096–1100.

45 J. E. Del Bene, *J. Phys. Chem.*, 1988, **92**, 2874–2880.

46 C. A. Murray, A. Richards, A. R. Baker, D. Bond, L. D. Connor, S. J. Day, J. Filik, P. Holloway, K. Levik, R. Mercado, J. Potter, C. C. Tang, S. P. Thompson, J. E. Parker, L. Holland, M. Basham, R. O'Brien and S. Fisher, *CrystEngComm*, 2024, **26**, 753–763.

47 CCDC 2404113: Experimental Crystal Structure Determination, 2025, DOI: 10.5517/ccdc.csd.cc2lpp11.